

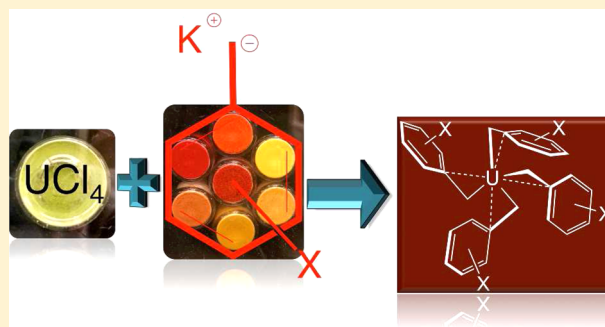
New Benzylpotassium Reagents and Their Utility for the Synthesis of Homoleptic Uranium(IV) Benzyl Derivatives

Sara A. Johnson, John J. Kiernicki, Phillip E. Fanwick, and Suzanne C. Bart*

H.C. Brown Laboratory, Department of Chemistry, Purdue University, West Lafayette, Indiana 47907, United States

Supporting Information

ABSTRACT: A new family of benzylpotassium reagents, KBn' ($\text{1-Bn}'$) ($\text{Bn}' = p\text{-}^i\text{PrBn}, p\text{-}^t\text{BuBn}, p\text{-NMe}_2\text{Bn}, p\text{-SMeBn}, m\text{-OMeBn}, o\text{-OMeBn}, 2\text{-picolyl}$), was synthesized using a modified literature procedure and characterized by multinuclear NMR spectroscopy. Combining four equivalents of $\text{1-Bn}'$ with UCl_4 at low temperature in THF afforded the homoleptic uranium(IV) derivatives $\text{2-Bn}'$ ($\text{2-}p\text{-}^i\text{Pr}, \text{2-}p\text{-}^t\text{Bu}, \text{2-}p\text{-NMe}_2, \text{2-}p\text{-SMe}, \text{2-}o\text{-Picolyl}, \text{2-}m\text{-OMe}, \text{2-}o\text{-OMe}$). In addition to ^1H NMR spectroscopic characterization, structural studies of five of these organouranium compounds ($\text{2-}p\text{-}^i\text{Pr}, \text{2-}p\text{-}^t\text{Bu}, \text{2-}o\text{-Picolyl}, \text{2-}m\text{-OMe}, \text{2-}o\text{-OMe}$) were performed, showing that in many cases the benzyl groups are coordinated in an η^4 -fashion, lending stability to these otherwise low-coordinate molecules. In the cases of $\text{U}(o\text{-OMeBn})_4$ ($\text{2-}o\text{-OMe}$) and $\text{U}(2\text{-picolyl})_4$ ($\text{2-}o\text{-Picolyl}$), heteroatom coordination to the uranium center is observed.



INTRODUCTION

Metal alkyls serve as important intermediates in a variety of industrial¹ and biological² processes; thus, new synthetic routes are always desirable. Such species can be formed via organometallic processes, including oxidative addition and β -alkyl elimination, but salt metathesis using organolithium or Grignard reagents remains a popular method for installation of alkyl and aryl groups on metal centers.^{3,4} Less attention has been devoted to other alkali metals, specifically sodium and potassium, for their ability to install M–C bonds. Although these reagents tend to be more reducing than their lithium counterparts, the formation of insoluble NaX and KX salts is advantageous as compared to LiX salts, which have increased solubility in polar solvents typically required for organometallic synthesis.

Historically, the generation and isolation of tetra(alkyl) uranium species of the form UR_4 has been attempted using alkylolithiums, but was not successful due to instability of the products at temperatures above 0 °C.^{5,6} We recently demonstrated the utility of potassium alkyls, specifically benzylpotassium, KCH_2Ph , and its methylated derivatives, $\text{KCH}_2\text{-}p\text{-CH}_3\text{C}_6\text{H}_4$ ⁷ and $\text{KCH}_2\text{-}m\text{-(CH}_3)_2\text{C}_6\text{H}_3$,⁸ in the synthesis of the first thermally stable neutral homoleptic uranium(IV) benzyl compounds.⁹ Treating UCl_4 with four equivalents of each of these salts at -108 °C (frozen THF) resulted in formation and isolation of the corresponding uranium products, $\text{U}(\text{CH}_2\text{Ph})_4$ (2-Bn), $\text{U}(\text{CH}_2\text{-}p\text{-CH}_3\text{C}_6\text{H}_4)_4$, and $\text{U}(\text{CH}_2\text{-}m\text{-(CH}_3)_2\text{C}_6\text{H}_3)_4$, in moderate yields. These reactions proceeded cleanly with elimination of KCl during workup with diethyl ether.⁹ In the case of 2-Bn and its derivatives, stability is imparted by the η^4 -coordination of the

benzyl groups, which prevent unwanted side reactions that have plagued previous synthetic attempts.^{5,6,10}

The successful isolation and characterization of 2-Bn demonstrated that perhaps this synthetic route could be expanded to produce organouranium species with alkyl-substituted benzyls, benzyls with functional groups, and 2-picoline. Along these lines, we targeted a general procedure to synthesize a new family of substituted benzylpotassium reagents, $\text{1-Bn}'$ ($\text{Bn}' = p\text{-}^i\text{PrBn}, p\text{-}^t\text{BuBn}, p\text{-NMe}_2\text{Bn}, p\text{-SMeBn}, m\text{-OMeBn}, o\text{-OMeBn}, 2\text{-picolyl}$), which would provide diversity in steric, electronic, and coordination environments for the resulting uranium complexes. Four members feature benzyl groups substituted in the *para* position with electron-donating groups, specifically ^iPr , ^tBu , NMe_2 , and SMe . Methoxy derivatives are substituted in both the *ortho* and *meta* positions, while the picolyl group has the nitrogen in the *ortho* position.

Given the variety of benzyl substituents, the synthesis for the potassium salts, $\text{1-Bn}'$, needs to be tolerant of functional groups and easy to perform while generating appreciable quantities. Since the original report of benzylpotassium by Gilman in the 1940s, many variations on its synthesis have been described. One of the earliest, which avoided the use of potassium metal, was that by Lochmann, who reported that addition of an alkylolithium to a solution of potassium (–)-(1R)-menthoxide was stirred at “a chosen temperature for the appropriate time”.¹¹ This procedure was a significant improvement over the previously reported synthesis for benzylpotassium, which involved treating potassium metal with organomercury

Received: March 13, 2015

Published: May 27, 2015

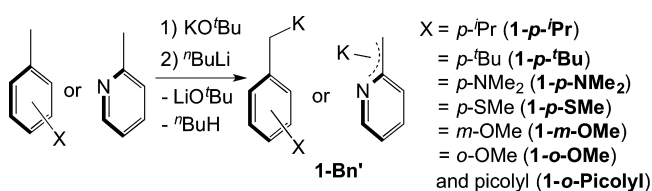
compounds.¹² From this work stemmed the advancement reported by Schlosser, who determined that commercially available potassium *tert*-butoxide and *n*-butyllithium could be combined with toluene to generate benzylpotassium cleanly.¹³

By eliminating elevated temperatures and potassium metal, Schlosser's procedure creates milder reaction conditions that are amenable for functionalized toluenes. Thus, herein we present a general synthesis for substituted benzylpotassium reagents, **1-Bn'**, by adaptation of this method, along with the characterization of these salts by multinuclear NMR spectroscopy. We also report the utility of **1-Bn'** in the generation of homoleptic uranium(IV) benzyl compounds, **2-Bn'**, which are significant given the rarity of neutral homoleptic uranium alkyls. These organouranium species have been fully characterized using ¹H NMR and electronic absorption spectroscopic methods, as well as by X-ray crystallography.

RESULTS AND DISCUSSION

The **1-Bn'** family was generated by freezing a slurry of KO^tBu and an excess of the substituted toluene reagent (*p*-ⁱPr, *p*-^tBu, *p*-NMe₂, *p*-SMe, *o*-OMe, *m*-OMe) or 2-picoline. Upon thawing, this solution was treated with a cooled solution of *n*-BuLi in hexanes, which instantly produced a color change to bright yellow or orange. Solutions were stirred at ambient temperature for the time given in Table 1, at which point conversion to deep

Table 1. Reaction Times and Abbreviations for **1-Bn'**



substituted toluene	reaction time (h)	abbreviation
CH ₃ - <i>p</i> - ⁱ Pr-C ₆ H ₄	3	1-p-ⁱPr
CH ₃ - <i>p</i> - ^t Bu-C ₆ H ₄	3	1-p-^tBu
CH ₃ -C ₆ H ₄ N	4	1-o-Picolyl
CH ₃ - <i>p</i> -NMe ₂ -C ₆ H ₄	2	1-p-NMe₂
CH ₃ - <i>p</i> -SMe-C ₆ H ₄	7	1-p-SMe
CH ₃ - <i>m</i> -OMe-C ₆ H ₄	12	1-m-OMe
CH ₃ - <i>o</i> -OMe-C ₆ H ₄	4	1-o-OMe

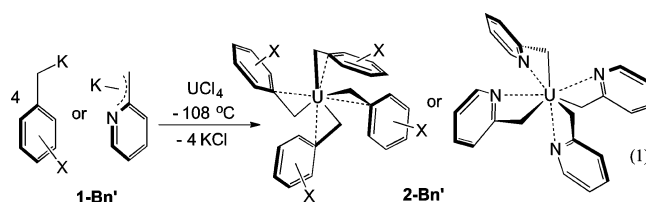
orange or yellow was noted. The substituted benzylpotassium reagents were collected as solids by filtration, washed thoroughly with pentane to remove LiO^tBu, and dried under vacuum.

Characterization of **1-Bn'** was possible by ¹H and ¹³C NMR spectroscopic analysis of THF-*d*₈ solutions of each (25 °C). For **1-p-ⁱPr**, **1-p-^tBu**, **1-p-NMe₂**, **1-p-SMe**, **1-m-OMe**, and **1-o-OMe**, the resonances for the methylenes were visible in the range 2–3 ppm (¹H) and 48–59 ppm (¹³C). The chemical shifts for additional resonances are presented in the Experimental Section. The ¹H and ¹³C NMR spectroscopic data for **1-o-Picolyl** compare well to previously acquired data, which showed an η³-azaallyl coordination mode with potassium.¹⁴ The purity of these salts was also assessed by elemental analysis. Attempts were made at the synthesis of the *p*-OMe variant; however, its instability precluded isolation and full characterization.¹⁵

A variation of Schlosser's procedure has already been reported for **1-o-Picolyl**¹⁶ and **1-p-^tBu**.¹⁷ However, we have

synthesized these according to the same conditions as for the rest of the **1-Bn'** family, as the previous procedure for **1-p-^tBu** requires potassium 3-methyl-3-pentanolate, which is not commercially available. The KO^tBu/ⁿBuLi method is also an improvement over that used to generate **1-o-OMe**,¹⁵ which was previously performed by ether cleavage of the benzylmethyl ether on a K mirror at –70 °C. Additionally, the synthesis for **1-m-OMe** was previously reported,¹⁵ but not accompanied by a repeatable detailed synthetic procedure.

With the new family of substituted benzylpotassium reagents in hand, attempts were made at the synthesis of the corresponding neutral homoleptic uranium(IV) benzyl derivatives, **2-Bn'**. By analogy to **2-Bn**, their synthesis using the **1-Bn'** family of salts was performed in frozen THF, and samples were not handled in solution at room temperature for prolonged periods. Mixing thawing THF solutions of UCl₄ and four equivalents of **1-Bn'** rapidly produced dark red or orange reaction mixtures. Volatiles were removed immediately, followed by workup in diethyl ether and filtration of KCl. The new uranium tetrabenzyls were isolated as dark red-brown solids in good yields and were stable in the solid state (eq 1).



Exceptions to this are **2-p-NMe₂** and **2-p-SMe**, which were found to decompose during workup. Successful synthesis of the **2-Bn'** family is significant, as substituted benzyl ligands on uranium are rare.

The organouranium products were analyzed by ¹H NMR spectroscopy (23 °C, benzene-*d*₆), and these data are presented in Table 2 along with a comparison of **2-Bn**. For the majority of

Table 2. ¹H NMR Spectroscopic Shifts for **2-Bn'** (C₆D₆, 23 °C)^a

benzyl-uranium	–CH ₂	<i>α</i> -CH
2-Bn	–30.41	–13.99 (<i>m</i>), 9.48 (<i>o</i>), 0.39 (<i>p</i>)
2-p-ⁱPr	–31.09	–13.20 (<i>m</i>), 9.40 (<i>o</i>)
2-p-^tBu	–32.07	–13.78 (<i>m</i>), 9.86 (<i>o</i>)
2-o-Picolyl	–32.21	16.15 (<i>m</i> -NCH or <i>o</i>), 9.19 (<i>m</i>) 4.84 (<i>m</i> -NCH or <i>o</i>), 4.94 (<i>p</i>)
2-p-NMe₂	–32.44	–11.56 (<i>m</i>), 8.46 (<i>o</i>)
2-p-SMe	–32.50	–13.78 (<i>m</i>), 9.84 (<i>o</i>)
2-m-OMe	–29.17	–19.23 (<i>o</i>), –14.77 (<i>o</i>), 0.09 (<i>p</i>), 9.40 (<i>m</i>)
2-o-OMe	4.16	–4.79 (<i>o</i>), 1.79, 5.79

^a*o* = *ortho*; *m* = *meta*, *p* = *para*.

the U(IV) complexes, the methylene protons have the most extreme chemical shifts due to their proximity to the paramagnetic uranium center, appearing between –29 and –33 ppm. The small range of chemical shifts for the methylene protons is not surprising given the similarity in electron-donating nature of the benzyl substituents. In the case of **2-o-OMe**, the methylene protons appear at 4.16, indicating a potentially different coordination mode than the rest of the family. For the complexes with *para* substitution, **2-p-ⁱPr**, **2-p-^tBu**, **2-p-NMe₂**, and **2-p-SMe**, equivalent resonances are noted for both the *ortho*- and *meta*-protons of the aryl rings.

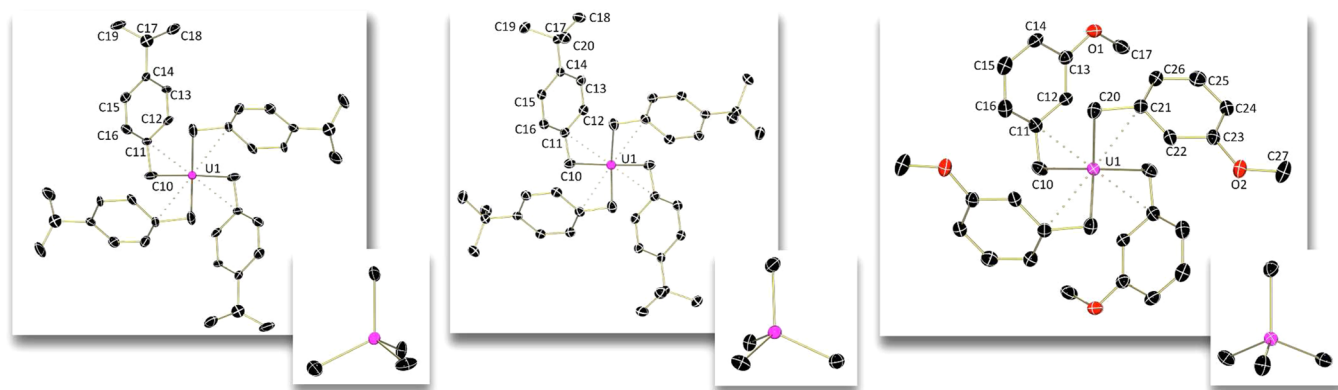


Figure 1. Molecular structures of **2-*p*-Pr** (left), **2-*p*-tBu** (center), and **2-*m*-OMe** (right) shown at 30% probability ellipsoids. H atoms, cocrystallized solvent molecules, and additional U–C bonds depicting η^4 -coordination have been omitted for clarity. Inset depicts geometry for sigma bonds to uranium.

Table 3. Structural Parameters for **2-*p*-Pr**, **2-*p*-tBu**, **2-*m*-OMe**, **2-*o*-OMe**, and **2-*o*-Picolyl**, with **2-Bn** for Comparison

	2-Bn	2-<i>p</i>-Pr	2-<i>p</i>-tBu	2-<i>m</i>-OMe	2-<i>o</i>-OMe	2-<i>o</i>-Picolyl
U–C bonds (Å)	2.446(7), 2.454(8), 2.477(7), 2.462(7)	2.438(19)	2.424(10)	2.450(5), 2.462(5)	2.446(8), 2.466(9)	2.555(5), 2.598(4), 2.611(4), 2.656(4)
U–C _{ipso} bonds (Å)	2.839(7), 2.762(7), 2.777(6), 2.700(8)	2.791(15)	2.792(9)	2.806(6), 2.772(6)	3.365, 3.356	2.818(4), 2.832(4), 2.834(4), 2.842(4)
U–C–C _{ipso} angles	89.4(4)°, 86.0(4)°, 85.7(4)°, 82.7(4)°	87.2(10)°	87.0(3)°	87.4(3)°, 86.4(4)°	114.7(5)°, 113.7(6)°	86.4(3)°, 84.3(2)°, 82.0(2)°, 84.1(2)°

The *ortho*-protons typically appear between 8 and 10 ppm, while those in the *meta* position show more variability, appearing between –11 and –14 ppm; these chemical shifts are as expected based on those for **2-Bn**. The rest of the family, **2-*o*-Picolyl**, **2-*m*-OMe**, and **2-*o*-OMe**, have *m*-CH resonances appearing within the same range, 8–10 ppm. The resonances for the *ortho*-protons, however, are quite shifted, appearing at 16.15 ppm for **2-*o*-Picolyl**, at –19.23 and –14.77 for **2-*m*-OMe**, and at –4.79 for **2-*o*-OMe**. While this resonance for **2-*o*-Picolyl** could not be definitively established based on integration value alone from the *meta* position, the assignment is proposed based on the chemical shift in the analogous species.

The isolation of **2-*p*-Pr**, **2-*p*-tBu**, **2-*m*-OMe**, **2-*o*-OMe**, and **2-*o*-Picolyl** expands the number of neutral homoleptic uranium(IV) alkyl compounds that have been characterized to eight (including **2-Bn**, U(CH₂-*p*-CH₃C₆H₄)₄ and U(CH₂-*m*-(CH₃)₂C₆H₃)₄). These species persist at ambient temperature, avoiding decomposition pathways. Typical breakdown of uranium alkyls includes U–C homolytic cleavage, which produces the corresponding substituted toluene or 2-picoline, and reductive elimination/radical coupling, both of which produce the substituted bibenzyl and are thus indistinguishable.^{5,10,18,19} To evaluate the relative stabilities of **2-*p*-Pr**, **2-*p*-tBu**, **2-*m*-OMe**, **2-*o*-OMe**, and **2-*o*-Picolyl**, the same method as for **2-Bn** was used.⁹ Benzene-*d*₆ solutions of each (with a ferrocene internal standard) at 23 °C were monitored by ¹H NMR spectroscopy over 3 days or until no starting material remained (Table S1). Following this, samples were filtered over a silica gel plug and washed with diethyl ether to remove uranium, without being subjected to vacuum. Solutions were analyzed by GC/MS to analyze the relative percentages of substituted toluenes and bibenzyls formed.

Previously, it was noted that decomposition of **2-Bn** occurred in approximately 6 h under these conditions, giving ~85%

toluene and ~15% bibenzyl.⁹ Both **2-*p*-Pr** and **2-*p*-tBu** were stable for over 24 h in solution, a significant improvement over **2-Bn**. **2-*p*-Pr** showed the same percentages as **2-Bn** for production of *p*-cymene and 4,4'-di-isopropylbibenzyl, whereas the **2-*p*-tBu** was slightly different at 84% 4-*tert*-butyltoluene and 16% 4,4'-di-*tert*-butylbibenzyl. The OMe-substituted compounds were both stable for less than 24 h, with the **2-*m*-OMe** producing >99% 3-methylanisole and trace 3,3'-ethylenebis(anisole), where **2-*o*-OMe** showed only 2-methylanisole and no 2,2'-ethylenebis(anisole) over the course of the experiment. In the case of **2-*o*-Picolyl**, only formation of 2-picoline was noted over the course of 1 h. The coupled product 2,2'-(1,2-ethanediyl)bis(pyridine) was not detected, likely due to the fact that dissociation of this chelate from the uranium center is unfavorable.

Following NMR spectroscopic analysis, electronic absorption spectroscopy was used to help elucidate the electronic structures of **2-Bn'**. Data for **2-Bn'** were collected from 380 to 2100 nm at ambient temperature in toluene (Figure S20). As expected, the spectra for the family are very similar. The UV–visible region has very broad transitions that are difficult to resolve. Broad, low-intensity bands assigned as Laporte-forbidden *f*–*f* transitions are found throughout the near-infrared region, as would be expected for uranium(IV) *f*² centers. These spectra are reminiscent of those noted for the (NN^R)U(CH₂Ph)₂ (NN^R = *fc*(NR)₂, *fc* = 1,1'-ferrocenediyl; R = Si^tBuMe₂, SiMe₃, SiMe₂Ph) family recently reported by Diaconescu.²⁰ Interestingly, lower molar absorptivities are noted in the spectra for **2-*o*-OMe** and **2-*o*-Picolyl** as compared to the rest of the family, perhaps indicating a difference in coordination of these ligands.

To establish the hapticity of the benzyl groups in **2-*p*-Pr**, **2-*p*-tBu**, **2-*m*-OMe**, **2-*o*-OMe**, and **2-*o*-Picolyl**, X-ray crystallography was used to evaluate bonding in these representative members of the family. On the basis of the analysis, the

Table 4. Comparison of the Structural Parameters for 2-*p*-^{*i*}Pr, 2-*p*-^{*t*}Bu, 2-*m*-OMe, and 2-Bn

	MC _{ipso} –MCH ₂ (Å)	MC _o –MCH ₂ (Å)	MC _{o'} –MCH ₂ (Å)	Δ ^a	Δ' ^b
2-Bn ⁹	0.39, 0.31 0.30, 0.24	0.95, 0.84 0.75, 0.71	0.98, 0.86 0.91, 0.83	0.56, 0.53 0.45, 0.47	0.59, 0.55 0.61, 0.59
2- <i>p</i> - ^{<i>i</i>} Pr	0.353	0.822	0.950	0.469	0.597
2- <i>p</i> - ^{<i>t</i>} Bu	0.368	0.836	1.054	0.468	0.686
2- <i>m</i> -OMe	0.344, 0.322	0.694, 0.642	1.034, 1.031	0.350, 0.320	0.690, 0.709

^aΔ = [MC_o–MCH₂] – [MC_{ipso}–MCH₂]. ^bΔ' = [MC_{o'}–MCH₂] – [MC_{ipso}–MCH₂].

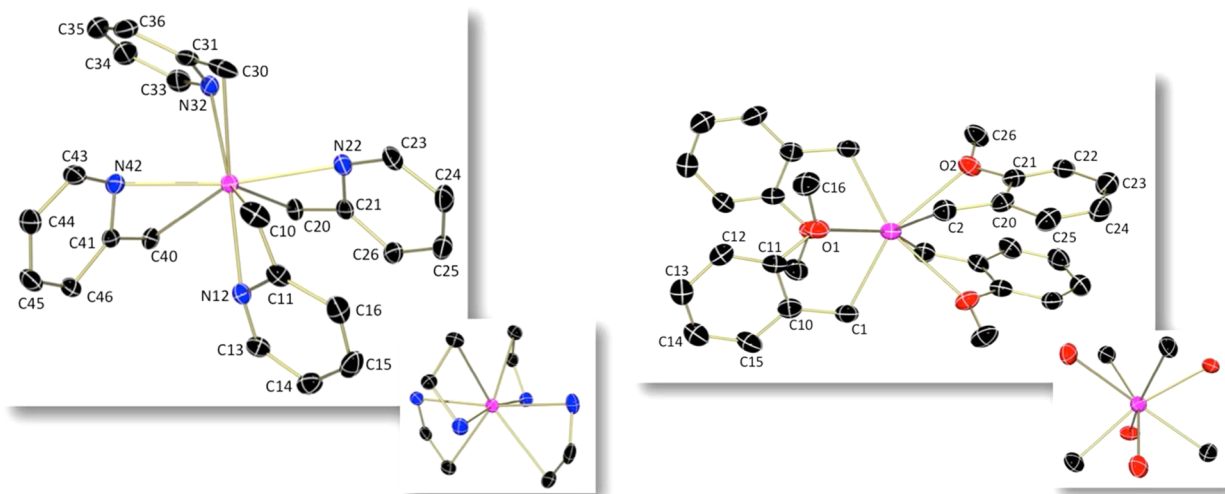


Figure 2. Molecular structures of 2-*o*-Picolyl (left) and 2-*o*-OMe (right) shown at 30% probability ellipsoids. Hydrogen atoms and cocrystallized solvent molecules have been omitted for clarity. Inset depicts geometry for sigma bonds to uranium.

homoleptic uranium(IV) compounds presented here can be divided into two groups: (1) those with *para* or *meta* substitution that have similar coordination geometries to 2-Bn and (2) those with divergent geometries due to heteroatom donation.

The members of the first category include 2-*p*-^{*i*}Pr, 2-*p*-^{*t*}Bu, and 2-*m*-OMe and were crystallized by cooling concentrated diethyl ether solutions to –35 °C; for 2-*p*-^{*i*}Pr, the solution was further layered with pentane to precipitate X-ray quality crystals. Analysis of each sample showed that both 2-*p*-^{*i*}Pr and 2-*p*-^{*t*}Bu are crystallographically symmetric with pseudo-tetrahedral geometries; thus their structural parameters are equivalent (Figure 1, structural parameters in Table 3). 2-*p*-^{*i*}Pr, 2-*p*-^{*t*}Bu, and 2-*m*-OMe have respective U–C σ -bond averages of 2.438(19), 2.424(10), and 2.456 Å, similar to 2-Bn (2.460(8) Å). Additionally, the distances to the *ipso*-carbon average 2.791(15), 2.792(9), and 2.789 Å, respectively, and are on the order of those observed for the parent species.

The hapticity of the benzyl substituents was established using parameters defined by Andersen for benzyluranium species, Δ and Δ', which are based on the U–C distances for the methylene (MCH₂), *ipso*- (MC_{ipso}), and *ortho*-carbons (MC_o is the shorter contact length, MC_{o'} is the longer contact length) of the benzyl groups.²¹ Thus, Δ = [MC_o–MCH₂] – [MC_{ipso}–MCH₂] and Δ' = [MC_{o'}–MCH₂] – [MC_{ipso}–MCH₂]. These data are tabulated for the 2-Bn' series presented here along with 2-Bn for comparison (Table 4). On the basis of the U–C distances for 2-*p*-^{*i*}Pr, 2-*p*-^{*t*}Bu, and 2-*m*-OMe, the calculated Δ and Δ' values, ranging from 0.320 to 0.469 and 0.597–0.709, respectively, support η^4 -benzyl coordination, as in the case of 2-Bn. This is also evident from the U–C–C angles that average 87.2(10)°, 87.0(3)°, and 86.9(4)° for 2-*p*-^{*i*}Pr, 2-

p-^{*t*}Bu, and 2-*m*-OMe, respectively, and compare well to that for 2-Bn (U–C–C_{av} = 86.0°).

The members of the second category, 2-*o*-Picolyl and 2-*o*-OMe, display coordination by an additional heteroatom in the *ortho* position and thus will be discussed individually. Crystals of 2-*o*-Picolyl were obtained by cooling a concentrated diethyl ether solution of this material layered with pentane to –35 °C. Analysis showed an eight-coordinate uranium center in 2-*o*-Picolyl, where all distances are crystallographically distinct (Figure 2, left, structural parameters in Table 3). The U–C σ -bond distances range from 2.555(5) to 2.656(4) Å, while those to the *ipso*-carbon of the phenyl group are ~2.8 Å. While the latter is on par with the compounds previously discussed, the σ -interaction is actually about 0.1 Å longer. The nitrogen atoms of the pyridine rings are coordinated, with U–N interactions averaging 2.452 Å, as expected for dative interactions. The U–N distances are on the order of those displayed in Cp*₂UMe(Spy) (2.448 Å)²² (py = pyridine) and Cp*₂U(η^2 -picoline)CH₃ (2.394(3) Å).²³ The coordination mode noted for 2-*o*-Picolyl is similar to that previously observed by Rothwell for the thorium(IV) species Th(OAr')₂(CH₂-py-6-Me)₂ (Ar' = 2,6-di-*tert*-butylphenyl).²⁴ In this molecule, the respective Th–C σ -bonds and Th–N distances of 2.55(1) and 2.61(1) Å are on the order of those for 2-*o*-Picolyl. Similarly, Kiplinger notes corresponding Th–C and Th–N distances of 2.642(10) and 2.574(7) Å in Cp*₂Th(CH₃)[η^2 -(N,C)-2-CH₂-NC₅H₃].²³ The M–C–C angles in 2-*o*-Picolyl range from 82.0(2)° to 86.4(3)°, as compared to 91.6(8)° for Th(OAr')₂(CH₂-py-6-Me)₂ and 87.9(5)° for Cp*₂Th(CH₃)[η^2 -(N,C)-2-CH₂-NC₅H₃]. As in both of these cases, the actinide lies out of the C–C–N plane of the pyridine ring, most likely in order to relieve steric pressure in the eight-coordinate species. While this decreases the nitrogen lone pair–metal overlap, this

decrease is insignificant compared to the relief from steric crowding that is gained.²⁴ Thus, the bonding in **2-*o*-Picolyl** is analogous to that noted for $\text{Cp}^*_2\text{Th}(\text{CH}_3)[\eta^2-(\text{N},\text{C})-2\text{-CH}_2\text{-NC}_5\text{H}_3]$, in which the metal–pyridine interaction can best be described as a distorted $\eta^2-(\text{C},\text{C}',\text{N})$ -azaallylic interaction.

The isolation and characterization of **2-*o*-Picolyl** is significant, as actinocenes with η^2 -picolyl ligands have been computationally determined as products in sp^3 C–H bond activation of 2-picoline and 2,6-lutidine.^{25,26} Such species have been isolated and characterized for thorium,²⁷ but not for uranium. The bond distances displayed by **2-*o*-Picolyl** are consistent with the calculations for $\text{Cp}^*_2\text{U}(\text{CH}_3)\eta^2-(\text{N},\text{C})-2\text{-CH}_2\text{-NC}_5\text{H}_4$, which has a U–C σ -bond distance of 2.598 Å and a U–N distance of 2.570 Å.²⁶

The second member of this family, **2-*o*-OMe**, was crystallized by cooling a concentrated THF/pentane solution to -35°C over 3 days. The solid-state structure as determined by X-ray diffraction shows a square antiprismatic uranium center, with each square composed of two carbon and two oxygen donors (Figure 2, right, structural parameters in Table 3). **2-*o*-OMe** is the first structurally characterized actinide compound to feature an *o*-OMe benzyl group; thus no direct comparisons to previous examples could be made for the U–O and U–C distances. **2-*o*-OMe** possesses a C_2 rotation axis, equivalencing the metrical parameters. The U–C distances of 2.446(8) and 2.466(9) Å are on the order of those of **2-*p*-Pr**, **2-*p*-Bu**, and **2-*m*-OMe**, but slightly shorter than those in **2-*o*-Picolyl**. The U–O distances of 2.671(5) and 2.672(5) Å are as expected for dative bonds to uranium.²⁸

Interesting structural features in **2-*o*-OMe** include the U–C–C angles of $114.7(5)^\circ$ and $113.7(6)^\circ$. These larger angles as compared to the rest of the compounds analyzed create a near-tetrahedral environment around the methylene carbons. This is not unexpected, given that there are no additional π interactions to uranium necessary, as **2-*o*-OMe** is coordinatively saturated. This is in contrast to **2-*p*-Pr**, **2-*p*-Bu**, and **2-*m*-OMe**, which maintain η^4 -bonding to prevent a sterically unsaturated four-coordinate species.

The generation of the neutral homoleptic uranium tetrabenzyl family presented here is an advance in understanding the fundamental organometallic chemistry of uranium. Previous synthetic attempts of four-coordinate uranium tetrabenzyl compounds were unsuccessful due to thermal instability. However, increasing the coordination number of the uranium center with additional π or heteroatom interactions imparts stability, allowing these species to be handled at ambient temperatures. Additionally, uranium complexes with these particular substituted benzyl groups have not previously been reported. Thus, these compounds mark new territory in the field of σ -bonded uranium alkyls.

CONCLUSIONS

In summary, a new family of benzylpotassium reagents has been synthesized using a modification of Schlosser's procedure and fully characterized. This has been accomplished in the absence of toxic precursors or deleterious side reactions. These reagents have been used for the synthesis of homoleptic uranium(IV) tetrabenzyl derivatives, as the **1-Bn'** reagents smoothly eliminate KCl in diethyl ether from UCl_4 . Characterization of these species by X-ray crystallography revealed that their inherent stability is due to the increased hapticity of the benzyl groups, which creates a saturated uranium center and slows unwanted decomposition reactions, including homolytic U–C

scission and β -hydrogen elimination. Thus, this family of uranium alkyls is significant, given the notorious instability of those tetraalkyls previously synthesized. Additionally, these benzyluranium compounds provide insight into the bonding and coordination modes of substituted benzyl ligands, as these have not been previously structurally characterized for actinides (except for 2-picoline). Future studies will be aimed at understanding fundamental organometallic reactions with these unique alkylated species.

EXPERIMENTAL SECTION

General Considerations. All air- and moisture-sensitive manipulations were performed using standard Schlenk techniques or in an MBraun inert atmosphere drybox with an atmosphere of purified nitrogen. The MBraun drybox was equipped with a coldwell designed for freezing samples in liquid nitrogen as well as two -35°C freezers for cooling samples and crystallizations. Solvents for sensitive manipulations were dried and deoxygenated using literature procedures with a Seca solvent purification system.²⁹ Benzene- d_6 was purchased from Cambridge Isotope Laboratories, dried with molecular sieves and sodium, and degassed by three freeze–pump–thaw cycles. THF- d_8 was purchased from Cambridge Isotope Laboratories and used as received. Potassium *tert*-butoxide and *n*-butyllithium (2.5 M in hexanes) were purchased from Sigma-Aldrich and used as received. Methyl *p*-tolyl sulfide, 4-*tert*-butyltoluene, *p*-cymene, 2-methylpyridine, and 4-methoxytoluene were purchased from Sigma-Aldrich and distilled from CaH_2 prior to use. Uranium tetrachloride was prepared according to literature procedures.³⁰

^1H NMR and ^{13}C NMR spectra were recorded on a Varian Inova 300 spectrometer operating at 299.992 and 75.424 MHz, respectively. All chemical shifts are reported relative to the peak for SiMe_4 , using ^1H (residual) chemical shifts of the solvent as a secondary standard. The spectra for paramagnetic molecules were obtained by using an acquisition time of 0.5 s; thus the peak widths reported have an error of ± 2 Hz. For paramagnetic molecules, the ^1H NMR data are reported with the chemical shift, followed by the peak width at half-height, the integration value, and, where possible, the peak assignment.

The capillary gas chromatography/mass spectrometry analyses were carried out with an Agilent 5975C (Agilent Laboratories, Santa Clara, CA, USA) mass spectrometer system. Typical electron energy was 70 eV with the ion source temperature maintained at 250°C . The individual components were separated by using a 30 m HP-5 capillary column ($250\text{ }\mu\text{m}$ i.d. \times $0.25\text{ }\mu\text{m}$ film thickness). The initial column temperature was set at 35°C (for 3 min) and programmed to reach 280°C with a ramp of $10.0^\circ\text{C}/\text{min}$. The flow rate was set at $1\text{ mL}/\text{min}$, and the injector was set at 250°C . Samples were run through a silica gel plug to remove uranium from organics in preparation for gas chromatography/mass spectrometry analysis.

Single crystals of **2-*o*-Picolyl** suitable for X-ray diffraction were coated with poly(isobutylene) oil in a glovebox and quickly transferred to the goniometer head of a Nonius KappaCCD image plate diffractometer equipped with a graphite crystal, incident beam monochromator. Preliminary examination and data collection were performed with Mo $K\alpha$ radiation ($\lambda = 0.71073\text{ Å}$). Single crystals of **2-*p*-Pr**, **2-*p*-Bu**, **2-*m*-OMe**, and **2-*o*-OMe** suitable for X-ray diffraction were coated with poly(isobutylene) oil in a glovebox and quickly transferred to the goniometer head of a Rigaku Rapid II image plate diffractometer equipped with a MicroMax002+ high-intensity copper X-ray source with confocal optics. Preliminary examination and data collection were performed with Cu $K\alpha$ radiation ($\lambda = 1.54184\text{ Å}$). Cell constants for data collection were obtained from least-squares refinement. The space group was identified using the program XPREP.³¹ The structures were solved using the structure solution program PATTY in DIRDIF99.³² Refinement was performed on a LINUX PC using SHELX-97.³¹

General Synthesis of Organopotassium Reagents. A modified procedure for organopotassium reagents, reported by Schlosser,¹³ was used to generate the series of organopotassium reagents. A 250 mL

round-bottom flask was charged with 2.00 g (17.8 mmol) of KO^tBu and excess substituted toluene (100 mL). The slurry was cooled in the coldwell for ~20 min or until frozen. While stirring, cold (−35 °C) *n*-butyllithium (2.5 M in hexanes) (7.12 mL, 17.8 mmol) was added to the thawing slurry, producing an immediate color change to yellow-orange. The solution was allowed to warm to room temperature for 1 to 20 h (see Table 1 for specific reaction times), at which point the mixture darkened to deep orange-red. The orange or yellow solid was collected using a fritted funnel and washed with a continuous stream of pentane totaling approximately ~200 mL to remove any remaining substituted toluene and LiO^tBu. The solid was dried on the vacuum line. Quantitative yields were obtained for all organopotassium reagents.

Reaction Times and Characterization for Organopotassium Reagents. 1-*p*-ⁱPr. After stirring for 2–3 h a bright orange solid was produced. Anal. Calcd for C₁₀H₁₃K: C, 69.70; H, 7.60. Found: C, 69.53; H, 7.44. ¹H NMR (THF-*d*₈, 25 °C): δ = 1.20 (d, 6H, ⁱPr-CH₃, *J* = 6.9 Hz), 2.26 (s, 2H, CH₂), 2.83 (septet, 1H, ⁱPr-CH, *J* = 7.0 Hz), 7.0–7.1 (m, 4H, CH). ¹³C NMR (THF-*d*₈, 25 °C): δ = 33.78 (ⁱPr-CH₃), 34.70 (ⁱPr-CH), 48.21 (CH₂), 110.40 (CH), 115.92 (C_{para}), 128.29 (CH), 152.64 (C_{ipso}).

1-*p*-^tBu. After stirring for 2–3 h a bright orange solid was produced. Anal. Calcd for C₁₁H₁₅K: C, 70.91; H, 8.11. Found: C, 70.83; H, 7.96. ¹H NMR (THF-*d*₈, 25 °C): δ = 1.06 (s, 3H, ^tBu-CH₃), 2.04 (s, 2H, CH₂), 5.54 (d, 2H, CH, *J* = 8.6 Hz), 6.15 (d, 2H, CH, *J* = 8.5 Hz). ¹³C NMR (THF-*d*₈, 25 °C): δ = 32.71 (Me), 33.63 (C_{ortho}), 48.19 (CH₂), 110.50 (C_{ortho}), 118.21 (C_{para}), 127.22 (C_{meta}), 152.21 (C_{ipso}).

1-*o*-Picolyl. After stirring for 3–4 h a bright yellow solid was produced. NMR data matched previously published data.¹⁴

1-*p*-NMe₂. After 1–2 h a bright orange-red solid was produced. Anal. Calcd for C₉H₁₂NK: C, 62.38; H, 6.98; N, 8.08. Found: C, 62.14; H, 6.87; N, 8.01. ¹H NMR (THF-*d*₈, 25 °C): δ = 2.17 (s, 2H, CH₂), 2.83 (s, 6H, CH₃), 6.60 (d, 2H, CH, *J* = 8.5 Hz), 6.92 (d, 2H, CH, *J* = 8.5 Hz). ¹³C NMR (THF-*d*₈, 25 °C): δ = 46.28 (CH₂), 46.60 (Me), 110.68 (CH), 123.28 (CH), 128.53 (C_{ipso}), 152.51 (C_{para}).

1-*p*-SMe. After 6–7 h a light orange solid was produced. Anal. Calcd for C₈H₉SK: C, 54.50; H, 5.14. Found: C, 54.32; H, 4.93. ¹H NMR (THF-*d*₈, 25 °C): δ = 1.93 (s, 3H, SMe-CH₃), 2.44 (s, 2H, CH₂), 5.44 (d, 2H, CH₂, *J* = 8.7 Hz), 6.14 (d, 2H, CH₂, *J* = 8.6 Hz). ¹³C NMR (THF-*d*₈, 25 °C): δ = 24.25 (Me), 58.91 (CH₂), 112.24 (CH), 130.28 (C_{ipso}), 137.39 (CH), 151.23 (C_{para}).

1-*m*-OMe. After 10–12 h a golden yellow solid was produced. Anal. Calcd for C₈H₉OK: C, 59.96; H, 5.66. Found: C, 59.78; H, 5.74. ¹H NMR (THF-*d*₈, 25 °C): δ = 2.28 (s, 2H, CH₂), 3.72 (s, 3H, OMe-CH₃), 6.65–6.70 (m, 3H, CH), 7.09 (t, 1H, CH, *J* = 7.9 Hz). ¹³C NMR (THF-*d*₈, 25 °C): δ = 53.49 (Me), 54.16 (CH₂), 83.73 (C_{ipso}), 92.99 (C_{meta}), 105.98 (CH), 130.57 (CH), 153.81 (CH), 163.14 (CH).

1-*o*-OMe. After 3–4 h a bright yellow solid was produced. Anal. Calcd for C₈H₉OK: C, 59.96; H, 5.66. Found: C, 59.30; H, 5.78. ¹H NMR (THF-*d*₈, 25 °C): δ = 0.99 (s, 2H, CH₂), 3.57 (s, 3H, OMe-CH₃), 4.63 (t, 1H, CH, *J* = 6.8 Hz), 5.85 (d, 1H, CH, *J* = 7.8 Hz), 5.94–5.99 (m, 2H, CH, *J* = 7.4 Hz). ¹³C NMR (THF-*d*₈, 25 °C): δ = 37.40 (C_{ortho}), 44.33 (CH₂), 55.74 (Me), 67.86 (CH), 95.24 (C_{ipso}), 112.27 (CH), 112.93 (CH), 124.86 (CH), 145.71 (CH).

General Synthesis for U(IV) Tetra(alkyls). A 20 mL scintillation vial was charged with 0.050 g (0.132 mmol) of UCl₄ and ~2 mL of THF and frozen in a coldwell. A second 20 mL scintillation vial was charged with 4 equiv (0.528 mmol) of organopotassium reagent and 2 mL of THF and frozen in a coldwell. The two solutions were combined and stirred while thawing, creating a dark red-brown solution. Volatiles were promptly removed *in vacuo*. The residue was taken up in diethyl ether and filtered to remove KCl. Immediate removal of the diethyl ether *in vacuo* left a red-brown solid.

Characterization for U(IV) Tetra(alkyls). 2-*p*-ⁱPr. A 0.091 g amount of 1-*p*-ⁱPr was added (51% yield). Single crystals suitable for X-ray crystallography were grown in concentrated diethyl ether layered with pentane at −35 °C overnight. Anal. Calcd for C₄₀H₅₂U: C, 62.32; H, 6.80. Found: C, 62.19; H, 6.82. ¹H NMR (C₆D₆, 25 °C): δ = −31.09 (43, 8H, CH₂), −13.20 (21, 8H, *m*-CH), 1.77 (7, 24H, ⁱPr-CH₃), 5.88 (14, m, 4H, ⁱPr-CH), 9.40 (12, 8H, *o*-CH).

2-*p*-^tBu. A 0.099 g amount of 1-*p*-^tBu was added (83% yield). Single crystals suitable for X-ray crystallography were grown in concentrated diethyl ether at −35 °C for 2 days. Anal. Calcd for C₄₄H₆₀U: C, 63.90; H, 7.31. Found: C, 63.72; H, 7.40. ¹H NMR (C₆D₆, 25 °C): δ = −32.09 (33, 8H, CH₂), −13.78 (22, 8H, *m*-CH), 1.82 (6, s, 36H, ^tBu-CH₃), 9.86 (13, 8H, *o*-CH).

2-*o*-Picolyl. A 0.070 g amount of 1-*o*-Picolyl was added (62% yield). Single crystals suitable for X-ray crystallography were grown in concentrated diethyl ether layered with pentane at −35 °C for 5 days. Due to the limited stability of the compound, elemental analysis was unable to be obtained. ¹H NMR (C₆D₆, 25 °C): δ = −32.21 (34, s, 8H, CH₂), 4.84 (d, 4H, *o*-CH or N-CH, *J* = 8.1 Hz), 4.94 (t, 4H, *p*-CH, *J* = 5.9 Hz), 9.19 (t, 4H, *m*-CH, *J* = 7.2 Hz), 16.15 (13, 4H, *o*-CH or N-CH).

2-*p*-NMe₂. A 0.093 g amount of 1-*p*-NMe₂ was added. Compound decomposes quickly upon workup. Therefore, crystals could not be grown for X-ray crystallography, and elemental analysis and yields could not be determined. ¹H NMR (C₆D₆, 25 °C): δ = −32.44 (3, 8H, CH₂), −11.56 (28, 8H, *m*-CH), 4.06 (4, 24H, NMe₂-CH₃), 8.46 (93, 8H, *o*-CH).

2-*p*-SMe. A 0.093 g amount of 1-*p*-SMe was added. Compound decomposes quickly upon workup. Therefore, crystals could not be grown for X-ray crystallography, and elemental analysis and yields could not be determined. ¹H NMR (C₆D₆, 25 °C): δ = −32.05 (42, 8H, CH₂), −13.78 (21, 8H, *m*-CH), 1.25 (6, 12H, SMe-CH₃), 9.84 (12, 8H, *o*-CH).

2-*m*-OMe. A 0.085 g amount of 1-*m*-OMe was added (67% yield). Single crystals suitable for X-ray crystallography were grown in concentrated diethyl ether at −35 °C for 3 days. Anal. Calcd for C₃₂H₃₆O₄U: C, 53.19; H, 5.02. Found: C, 52.96; H, 4.94. ¹H NMR (C₆D₆, 25 °C): δ = −29.17 (29, 8H, CH₂), −19.23 (67, 4H, *o*-CH), −14.77 (241, 4H, *o*-CH), 0.09 (5, d, 4H, *p*-CH, *J* = 8.1 Hz), 1.17 (4, 12H, OMe-CH₃), 9.40 (77, 4H, *m*-CH).

2-*o*-OMe. A 0.085 g amount of 1-*o*-OMe was added (71% yield). Single crystals suitable for X-ray crystallography were grown in concentrated THF and pentane at −35 °C for 3 days. Anal. Calcd for C₃₂H₃₆O₄U: C, 53.19; H, 5.02. Found: C, 52.89; H, 4.87. ¹H NMR (C₆D₆, 25 °C): δ = −4.79 (6, 4H, CH), −4.76 (7, 12H, OMe-CH₃), −1.79 (t, 4H, CH, *J* = 7.4 Hz), 4.16 (45, 8H, CH₂), 5.79 (t, 4H, CH, *J* = 7.3 Hz), 6.92 (d, 4H, CH, *J* = 7.8 Hz).

■ ASSOCIATED CONTENT

Supporting Information

Multinuclear NMR spectra, X-ray crystallographic experiments, electronic absorption data, and table of decomposition data. The Supporting Information is available free of charge on the ACS Publications website at DOI: 10.1021/acs.organomet.5b00212.

■ AUTHOR INFORMATION

Corresponding Author

*E-mail: sbart@purdue.edu.

Notes

The authors declare no competing financial interest.

■ ACKNOWLEDGMENTS

We acknowledge the National Science Foundation (CAREER grant to S.C.B., CHE-1149875) for funding.

■ REFERENCES

- (1) Hoff, R.; Mathers, R. *Handbook of Transition Metal Polymerization Catalysts*; Wiley: Hoboken, 2010.
- (2) Sigel, H.; Sigel, A. *Biological Properties of Metal Alkyl Derivatives*; Marcel Dekker: New York, 1993.
- (3) Crabtree, R. H. *The Organometallic Chemistry of the Transition Metals*, 4th ed.; Wiley-Interscience: Hoboken, 2005.

- (4) Hartwig, J. F. *Organotransition Metal Chemistry: From Bonding to Catalysis*; University Science Books, 2010.
- (5) Marks, T. J.; Seyam, A. M. *J. Organomet. Chem.* **1974**, 67, 61–66.
- (6) Seyam, A. M. *Inorg. Chim. Acta* **1983**, 77, L123–L125.
- (7) Bambirra, S.; Meetsma, A.; Hessen, B. *Organometallics* **2006**, 25, 3454–3462.
- (8) Bailey, P. J.; Coxall, R. A.; Dick, C. M.; Fabre, S.; Henderson, L. C.; Herber, C.; Liddle, S. T.; Loroño-Gonzalez, D.; Parkin, A.; Parsons, S. *Chem.—Eur. J.* **2003**, 9, 4820–4828.
- (9) Kraft, S. J.; Fanwick, P. E.; Bart, S. C. *J. Am. Chem. Soc.* **2012**, 134, 6160–6168.
- (10) Marks, T. J.; Seyam, A. M. *J. Am. Chem. Soc.* **1972**, 94, 6545–6546.
- (11) Lochmann, L.; Lim, D. J. *Organomet. Chem.* **1971**, 28, 153–158.
- (12) Schlosser, M. *Angew. Chem., Int. Ed. Engl.* **1964**, 3, 287–306.
- (13) Schlosser, M.; Hartmann, J. *Angew. Chem., Int. Ed. Engl.* **1973**, 12, 508–509.
- (14) Kennedy, A. R.; Mulvey, R. E.; Urquhart, R. I.; Robertson, S. D. *Dalton Trans.* **2014**, 43, 14265–14274.
- (15) Vanermen, G.; Van Beylen, M.; Geerlings, P. *J. Phys. Chem.* **1986**, 90, 603–607.
- (16) Kim, Y. H.; Kim, T. H.; Kim, N. Y.; Cho, E. S.; Lee, B. Y.; Shin, D. M.; Chung, Y. K. *Organometallics* **2003**, 22, 1503–1511.
- (17) Harder, S.; Mueller, S.; Huebner, E. *Organometallics* **2004**, 23, 178–183.
- (18) Marks, T. J.; Seyam, A. M.; Kolb, J. R. *J. Am. Chem. Soc.* **1973**, 95, 5529–5539.
- (19) Davidson, P. J.; Lappert, M. F.; Pearce, R. *Chem. Rev.* **1976**, 76, 219–242.
- (20) Duhovic, S.; Oria, J. V.; Odoh, S. O.; Schreckenbach, G.; Batista, E. R.; Diaconescu, P. L. *Organometallics* **2013**, 32, 6012–6021.
- (21) Edwards, P. G.; Andersen, R. A.; Zalkin, A. *Organometallics* **1984**, 3, 293–298.
- (22) Evans, W. J.; Walensky, J. R.; Ziller, J. W. *Inorg. Chem.* **2010**, 49, 1743–1749.
- (23) Kiplinger, J. L.; Scott, B. L.; Schelter, E. J.; Pool Davis Tournear, J. A. *J. Alloys Compd.* **2007**, 444–445, 477–482.
- (24) Beshouri, S. M.; Fanwick, P. E.; Rothwell, I. P.; Huffman, J. C. *Organometallics* **1987**, 6, 2498–2502.
- (25) Castro, L.; Yahia, A.; Maron, L. *Dalton Trans.* **2010**, 39, 6682–6692.
- (26) Yang, P.; Warnke, I.; Martin, R. L.; Hay, P. J. *Organometallics* **2008**, 27, 1384–1392.
- (27) Pool, J. A.; Scott, B. L.; Kiplinger, J. L. *J. Alloys Compd.* **2006**, 418, 178–183.
- (28) Avens, L. R.; Bott, S. G.; Clark, D. L.; Sattelberger, A. P.; Watkin, J. G.; Zwick, B. D. *Inorg. Chem.* **1994**, 33, 2248–2256.
- (29) Pangborn, A. B.; Giardello, M. A.; Grubbs, R. H.; Rosen, R. K.; Timmers, F. J. *Organometallics* **1996**, 15, 1518–1520.
- (30) Kiplinger, J. L.; Morris, D. E.; Scott, B. L.; Burns, C. J. *Organometallics* **2002**, 21, 5978–5982.
- (31) Sheldrick, G. M. *Acta Crystallogr.* **2008**, A64, 112–122.
- (32) Beurskens, P. T.; Beurskens, G.; De Gelder, R.; Garcia-Granda, S.; Gould, R. O.; Smits, J. M. M. *Dirdif2008 Program System*; Crystallography Laboratory, University of Nijmegen: The Netherlands, 2008.